Mechanical and Morphological Characteristics of Poly(vinyl alcohol)/Chitosan Hydrogels

D. T. Mathews,[1,2] Y. A. Birney,[2] P. A. Cahill,[2] G. B. McGuinness[1]

[1]*School of Mechanical and Manufacturing Engineering, Dublin City University, Dublin 9, Ireland*
[2]*Vascular Health Research Centre, Dublin City University, Dublin 9, Ireland*

Received 12 October 2007; accepted 11 January 2008
DOI 10.1002/app.28104
Published online 15 April 2008 in Wiley InterScience (www.interscience.wiley.com).

ABSTRACT: The effect of freeze–thaw cycles and chitosan type (water-soluble or insoluble) on the morphological and mechanical characteristics of poly(vinyl alcohol) (PVA)/chitosan hydrogels was investigated with scanning electron microscopy (SEM), uniaxial testing, and a biaxial tubular vessel inflation experiment. SEM images showed that although multiple freeze–thaw cycles had no significant effect on pore size for PVA hydrogels without chitosan, both types of PVA–chitosan hydrogel developed a more porous structure with a greater distribution of pore size. Uniaxial mechanical tests demonstrated decreasing elasticity for successive freeze–thaw cycles within a range comparable to porcine aortic tissue. A conditioning effect, which modified the elastic response of the hydrogels after the first loading cycle, was also shown. Coefficients for hyperelastic material models were determined for the PVA–chitosan (water-soluble) hydrogels. The internal pressurization and axial extension of a tubular vessel within the physiological range was investigated experimentally and compared with the predictions of a numerical model. © 2008 Wiley Periodicals, Inc. J Appl Polym Sci 109: 1129–1137, 2008

Key words: biomaterials; blends; hydrogels; macroporous polymers; stress

INTRODUCTION

There has been much recent interest in the use of various hydrogels for vascular cell culture, encapsulation, and tissue engineering applications. To create functional tissue through engineering, a biomaterial that permits cell signaling is required.[1] For cells to function properly, appropriate signals are required, which may include chemical signals (growth factors) or mechanical signals (shear stress or hydrostatic pressure).[1] In addition, the biomaterial should provide a binding surface for the cells. There are currently a broad range of both natural and synthetic biomaterials used to produce substrates for a range of applications.

Hydrogels are water-swollen crosslinked polymer networks, which often exhibit characteristics, such as tissuelike elasticity and mechanical strength, that can be engineered for the application of choice,[2] and the appearance and feel of poly(vinyl alcohol) (PVA) hydrogels are similar to those of native arterial tissue. Chu and Rutt[3] developed PVA arterial vessels with similar mechanical properties to those of porcine aortas.

Synthetic constituents such as PVA can provide alternatives to natural materials and offer some advantages. They can be produced with excellent reproducibility and reliability through consistent protocols and a reliable materials source.[4] The mechanical properties of these constituents may be engineered for specific applications.[2] To promote tissue cell growth on a biomaterial for use as a scaffold, the material must be highly porous.[5] However, an optimum pore size is required, as small pores sizes may affect nutrition and waste exchange by cells, whereas larger pores affect the stability of the scaffold and its ability to provide physical support for the seeded cells.[6] Synthetic constituents can also be customized to incorporate bioactive signals (e.g., fibronectin,[2] chitosan,[7] peptides[8,9]) that evoke desirable cellular responses.[1]

PVA hydrogels have been evaluated for many biomedical applications,[10] including arterial phantoms,[3] heart valves,[11,12] corneal implants,[13] and cartilage tissue substitutes.[14] PVA hydrogels may be formed by physical crosslinking with freeze–thaw cycles,[3,15] chemical crosslinking with aldehydes,[2] and ultraviolet radiation.[8] The crosslinking of PVA, the concentration of the aqueous solution, and the molecular weight of PVA can be manipulated to control properties such as the overall water content, mechanical strength, and diffusive properties of the hydrogel. Hassan et al.[16] demonstrated that as the number of freeze–thaw cycles increased, the rate and overall amount of dissolution of PVA decreased. It has also been shown for PVA hydrogels that as the number of freeze–thaw cycles increase, enhanced stability during swelling at 37°C for a 6-month period is

Correspondence to: G. B. McGuinness (garrett.mcguinness@dcu.ie).

Journal of Applied Polymer Science, Vol. 109, 1129–1137 (2008)

evident, which demonstrates their appropriateness for long-term biomedical applications.[16,17]

PVA hydrogels have hydrophilic properties.[2] Therefore, important cell adhesion proteins do not adsorb to PVA hydrogels, and as a result, cells are unable to adhere to the hydrogel. To improve the compatibility and cell adhesion characteristics of PVA, different biological macromolecules, such as collagen, hyaluronic acid, chitosan, fibronectin, and peptides, have been blended with PVA hydrogels.[5] Cascone et al.[5] investigated the morphology and porosity characteristics of PVA containing different concentrations of biological materials. They concluded that when a natural macromolecule is added to PVA, the internal structure and porosity of the hydrogel changes.

Chitosan is derived from chitin, a polysaccharide that is present in the hard exoskeletons of shellfish-like shrimp and crabs.[18] In its crystalline form, chitosan is insoluble in aqueous solutions above pH 7. However, in dilute acids (e.g., pH < 6.0), acetic acid solubility can be achieved. In a precursor to this study, we[19] demonstrated the attachment and growth of bovine aortic endothelial and smooth muscle cells on 6% PVA–0.4% chitosan (water-soluble and water-insoluble) hydrogels. Chitosan blended with PVA[7] was shown to support fibroblast cell growth. Chuang et al.[7] reported that PVA–chitosan blended membranes are more favorable for fibroblast cell culture than pure PVA membranes. Cultured cells displayed good spreading, cytoplasm webbing, and flattening.[7] Koyano et al.[20] showed that fibroblast cell attachment and growth on a PVA hydrogel with 40 wt % chitosan exceeded collagen in both quality of cell attachment and cell growth. The combination of good cell compatibility with the ability to bind to growth factors and to be processed into different shapes makes chitosan a promising candidate for tissue engineering applications.

In this study, the mechanical characterization of 6% PVA–0.4% chitosan (water-soluble and water-insoluble) hydrogels was conducted to ensure that appropriate tissuelike properties were exhibited by the modified hydrogels in membrane and tubular forms. The morphological characteristics of the fabricated hydrogels were investigated by scanning electron microscopy (SEM). These particular hydrogel compositions were selected for mechanical and morphological evaluation because they displayed excellent vascular cell adhesion, cell growth characteristics, and cell morphologies, as shown in our previous study.[19]

EXPERIMENTAL

Preparation of the polymer hydrogel

The polymer solutions were prepared and crosslinked as described in our previous article.[19] Briefly, a 10% PVA solution was prepared by the mixture of crystals with an average molecular weight of 78,400 g/mol (Vassar Brothers Medical Center, New York) with sterile distilled water and autoclaved for 1 h at 121°C. Water-insoluble chitosan powder with a molecular weight of 810,000 g/mol and an 85% degree of deacetylation (Sigma Aldrich, Poole, Dorset, England) was dissolved at a 1.0% concentration in an aqueous solution of 0.2*M* acetic acid. One percent concentrations of water-soluble chitosan with a deacetylation degree of 85% (Jinan Haidebi Marine Bioengineering Co., Ltd., Jinan City, China) were also primed. The water-insoluble and water-soluble chitosan solutions were each blended into a 10% PVA solution at a ratio of 3 : 2 and were sterilized by autoclaving at a temperature of 121°C for 30 min. The PVA–chitosan blended solutions were cast into Perspex molds (Access Plastics, Dublin, Ireland) to produce membranes for either uniaxial testing or tubular vessels.

To crosslink the PVA–water-soluble chitosan and PVA–water-insoluble chitosan solutions (designated WS-1 and IS-1, respectively) in their molds, the solutions were frozen at −20°C for 12 h and thawed for 12 h. After this, the PVA–chitosan samples were placed in a sterile coagulation bath (1 L of distilled H_2O, 75 g of KOH, and Na_2SO_4 to saturation) to crosslink the chitosan in the PVA–chitosan membrane.[7]

Uniaxial specimens

Uniaxial test specimens were prepared as discussed previously with a mold manufactured from Perspex to produce hydrogel sheets 2.5 mm thick. To ensure consistent shape and dimensions for all of the test specimens, a dogbone-shaped cutting device was designed and manufactured from stainless steel. The overall specimen size was 80×14 mm^2. Before the specimens were tested, the thickness of each piece was measured with a depth micrometer. The middle segment of the specimen had a uniform cross-sectional area and was assumed to undergo uniform reduction when the sample was subjected to tension. The hydrogel tensile specimens were placed in distilled water at room temperature before use for up to 1 week. Uniaxial tensile specimens were fabricated for the PVA–chitosan WS-1 and PVA–chitosan IS-1 solutions.

Tubular vessels

Tubular PVA–chitosan hydrogel vessels were fabricated (dimensions: length = 100 mm, outer diameter = 13.5 mm, thickness = 1.5 mm) with a mold designed and manufactured from Perspex. The dimensions were selected to be typical of the iliac

artery. To minimize the evaporation of water, the PVA–chitosan solution was minimally exposed to air, and the mold was sealed immediately after filling. It was stored vertically at room temperature for 1 h to allow air bubbles to rise out of the solution. After this, the PVA–chitosan solution was cross-linked with freeze–thaw cycles and the coagulation bath. The vessels were stored in a bath of distilled water at room temperature to prevent dehydration before use for up to 1 week.

Uniaxial test procedure

The uniaxial tensile tests were performed on a Zwick Z005 displacement-controlled tensile testing machine (Zwick Roell GmbH, Ulm, Germany). Stainless steel grips, the gripping faces of which were covered with emery paper to prevent slippage during loading, were mounted onto the tensile testing machine. The extension of the specimen was taken to be the crosshead displacement. All samples in the tests of this study were loaded until failure of the hydrogel specimen occurred. Tests were conducted on samples loaded to failure at a strain rate of 60%/min. Separately, a study of the conditioning effect of multiple loading cycles was conducted on selected specimens to predefined loads, also at a strain rate of 60%/min.

At the start of each test, the load was calibrated and balanced to zero. The gauge length was also set to zero at the beginning of each test. The tests were stopped when tearing began at either the grips or along the length of the specimen. Load, displacement, gauge length, and cross-sectional area were recorded for each specimen. We obtained the engineering stress (σ_E) by dividing the instantaneous load by the original cross-sectional area. We determined the engineering strain (ε_E) by dividing the change in length by the original length. The original length of each specimen was taken as the distance between the custom-made stainless steel grips. For the purposes of graphical presentation, the σ_E and ε_E values were converted to true stress (σ_T) and true strain (ε_T) values with the following equations:

$$\sigma_T = \sigma_E(1 + \varepsilon_E) \tag{1}$$

$$\varepsilon_T = \ln(1 + \varepsilon_E) \tag{2}$$

Constitutive model

Mathematical models from nonlinear elasticity can be used to represent the behavior of rubberlike materials and have been widely used to model arterial tissue mechanics. The uniaxial test results for the various hydrogel samples can be used to define coefficients for these mathematical models, to allow the prediction of behavior in more complex geometrical and loading conditions.

The Ogden model was formulated to model incompressible hyperelastic materials.[21] The Ogden form of the strain energy potential is based on the principal stretches (λ_i's) and has the following form:

$$W = \sum_{k=1}^{N} \frac{\mu_k}{\alpha_k}(\lambda_1^{-\alpha_k} + \lambda_2^{-\alpha_k} + \lambda_3^{-\alpha_k} - 3) \tag{3}$$

where W is the strain energy density, μ_k and α_k are the material constants established from experimental data fitting.

To determine the hyperelastic constants, μ_k and α_k of a two-parameter Ogden model, a nonlinear regression routine that is available from Marc/Mentat (MSC Software, Santa Ana, CA) was used to obtain the model that best fit the uniaxial data. During data fitting, the least squares error to be minimized was based on absolute errors.

Vessel inflation testing

A PVA–chitosan hydrogel vessel clamped at a constant length with a predefined axial strain was inflated by the application of an internal pressure. The apparatus consisted of a fabricated PVA–chitosan WS-1 hydrogel tubular sample that had undergone three freeze–thaw cycles, additional tubing, a low-pressure transducer (Jofra Calibrators, Farum, Denmark), a valve, and a pressure inflation device (Medtronic, Ireland) used to apply an internal pressure. The internal pressure was measured by the pressure transducer. Digital vernier calipers were used to measure the external diameter of the hydrogel vessel at internal pressures ranging from 0 to 16 kPa. Pressure versus diameter data was obtained for the PVA–chitosan WS-1 hydrogel tubes, which were subjected to axial strains of 0, 5, 10, and 20%, respectively.

The pressure versus diameter data acquired from this experimental setup was compared to the pressure versus diameter response of a finite element model of the hydrogel vessel simulated with the constitutive parameters determined for the three freeze–thaw cycle PVA–chitosan WS-1 hydrogel.

SEM

The cross-sectional structure of the PVA–chitosan blended hydrogels were examined with a Hitachi S 300N scanning electron microscope (Tokyo, Japan). The images were analyzed with SEM Image Analysis software (Oxford Instruments, Abingdon, Oxfordshire, UK).

Before SEM examination, the hydrated hydrogel samples were cut into squares (15×15 mm^2), frozen overnight at -80°C, and then freeze-dried in a Labconco Freeze Dry Freezone System (Labconco, Kansas city, MO) for 10 h. The dehydrated hydrogel

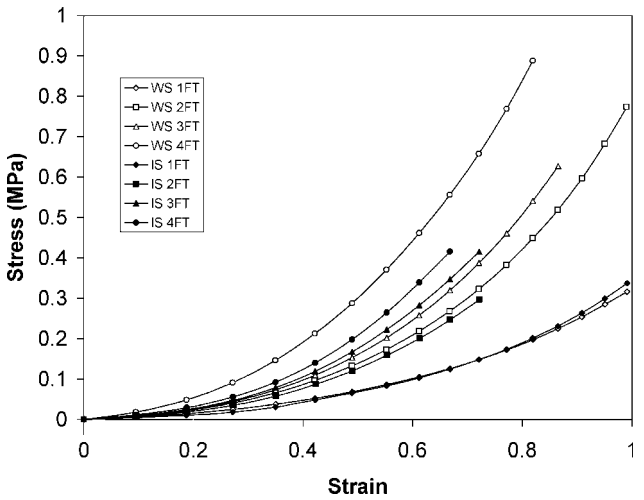

Figure 1 Uniaxial stress–strain data from the PVA–chitosan WS and IS hydrogel samples for one, two, three, and four freeze–thaw cycles.

specimens were placed in a minivice to examine the cross-sectional structure of the hydrogel. Samples were analyzed *in vacuo* and with an operating voltage of 20 kV. The effects of the blending of PVA with water-soluble and water-insoluble chitosan were investigated.

RESULTS AND DISCUSSION

Uniaxial tensile tests

The number of freeze–thaw cycles for PVA–chitosan IS-1 and PVA–chitosan WS-1 hydrogels was varied to determine any effect on the tensile behavior of the hydrogel. It is evident from Figure 1 that the number of freeze–thaw cycles had a pronounced effect on the elastic behavior of the various samples. The stiffness of each hydrogel increased as the number of freeze–thaw cycles increased, which was consistent with the known behavior of PVA hydrogels.

As shown in Figure 1, the PVA–chitosan IS and PVA–chitosan WS hydrogels displayed similar elastic behavior. A change in the elastic behavior of the PVA–chitosan IS and PVA–chitosan WS hydrogels was evident for each additional freeze–thaw cycle. However, in each case, the stress versus strain behavior for both hydrogels remained similar (Fig. 1).

It was shown by Chu and Rutt[3] that PVA stiffens as the number of freeze–thaw cycles is increased. This characteristic was also evident for the PVA–chitosan IS and PVA–chitosan WS hydrogels. For the PVA–chitosan IS and WS hydrogels, the PVA was again crosslinked during the freeze–thaw cycles. Although the chitosan was encapsulated in the PVA matrix, it would not have been crosslinked during the freeze–thaw cycles. The hydrogels were submerged in the coagulation bath to crosslink the chitosan and neutralize the pH (associated with the presence of acetic acid). The chitosan coagulation process is based on an acid–base reaction between the chitosan dissolved in acetic acid and the potassium hydroxide base. Knaul and Creber[22] discussed a similar process of the coagulation of chitosan in a strong basic solution (aqueous sodium hydroxide) brought about by proton exchange between acetic acid and a sodium hydroxide base.

With regard to the determination of the mechanical properties of the materials, the PVA was certainly the more mechanically significant component. Although the chitosan may have contributed to the mechanical properties, it was the effect of the freeze–thaw cycles on PVA that significantly affected the elastic behavior of the hydrogels. In addition to the crosslinking effect, there may have been further gelation of PVA in later freeze–thaw cycles, and this may have contributed to the stiffening of the hydrogel. Because the mold was subjected to repeated freeze–thaw cycles without the liquid solution being washed out, it is possible that gelation of some PVA in the second, third, or fourth cycle contributed to the freeze–thaw effect.

A comparison of the PVA–chitosan IS and PVA–chitosan WS hydrogels showed that the use of water-soluble or insoluble chitosan was insignificant for one, two, three, and four freeze–thaw cycles.

Constitutive model parameters

Table I shows the coefficients determined for the Ogden 2 parameter constitutive model on the basis

TABLE I
Hyperelastic Material Constants Describing PVA–Chitosan WS-1 for One, Two, Three, and Four Freeze–Thaw Cycles Based on Experimental Data from Uniaxial Tension Tests (Fig. 1)

Freeze–thaw cycles	μ_1 (kPa)	μ_2 (kPa)	α_1	α_2	Error
1	8.90	4.31×10^{-5}	6162.6	1716.9	5.63×10^{-4}
2	4.54	14.71	8075.1	4604.8	4.89×10^{-3}
3	13.97	8.65×10^{-8}	7076.4	5100.5	4.70×10^{-3}
4	3.42×10^{-5}	31.09	2633.1	6599.3	9.79×10^{-3}

The parameters describe a two-parameter Ogden model.

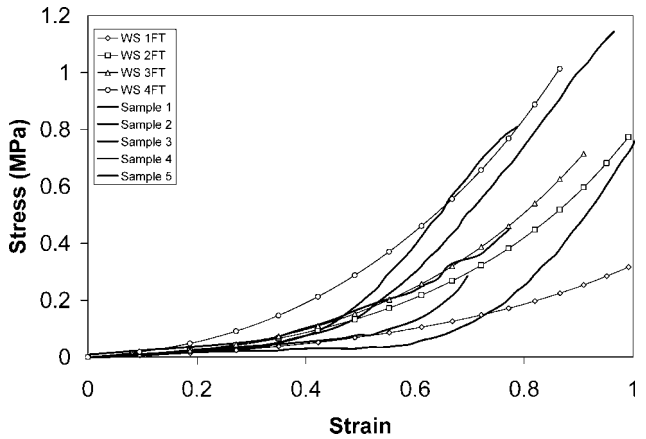

Figure 2 Uniaxial stress–strain data from the PVA–chitosan WS hydrogel samples that underwent one, two, three, and four freeze–thaw cycles versus five uniaxial stress–strain curves for porcine aortic tissue. Porcine data were digitized from Prendergast et al.[23] (with Xyextract digitizing software).

of the uniaxial experimental data for PVA–chitosan WS-1 that had undergone one, two, three, and four freeze–thaw cycles (Fig. 1).

Comparison of PVA–chitosan WS to porcine aorta

The uniaxial stress versus strain curves for the PVA–chitosan WS specimens for one, two, three, and four freeze–thaw cycles were compared to five published uniaxial stress versus strain curves for porcine aortic tissue.[23] Clearly, the PVA–chitosan WS samples bore a close resemblance to the porcine aortic tissue (Fig. 2). The PVA–chitosan WS membranes that experienced one, two, and three freeze–thaw cycles had similar stress versus strain characteristics within the 0–0.6 strain range. The hydrogel fabricated with four freeze–thaw cycles was stiffer compared to the uniaxial stress versus strain curves for all five porcine aortic samples. In common with pure PVA hydrogels, which were previously fabricated to match the constitutive response of porcine aortic tissue[3] and a human carotid artery,[24] the uniaxial stress versus strain characteristics for the PVA–chitosan WS membranes fabricated with one, two, and three freeze–thaw cycles closely resembled the uniaxial stress versus strain curves for porcine aortic tissue. One freeze–thaw cycle and three freeze–thaw cycles represented bounds on the softer and stiffer porcine aortic specimens, respectively.

Effect of multiple loading cycles

The hydrogel membranes were tested to determine whether there was any variation in the elastic behavior of the hydrogels during cyclic loading. Specimens

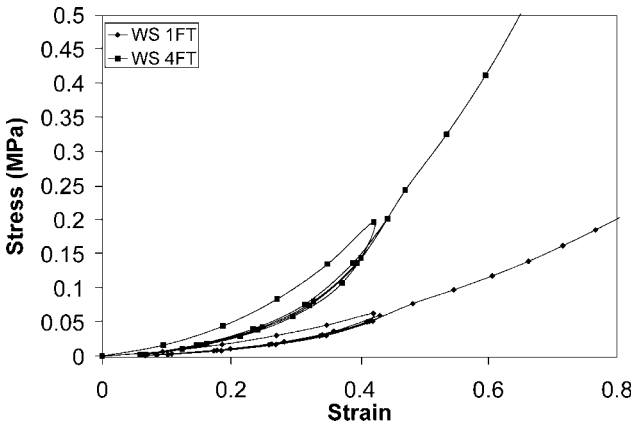

Figure 3 Two preconditioning cycles of PVA–chitosan WS to a load of 0.3 N, which was then loaded to failure (one and four freeze–thaw cycles).

of the PVA–chitosan IS and WS hydrogels that underwent one and four freeze–thaw cycles (plus coagulation bath) were subject to two consecutive loading–unloading cycles before they were tested to failure. Because of the variation in the stress versus strain relationships of the hydrogels subjected to one

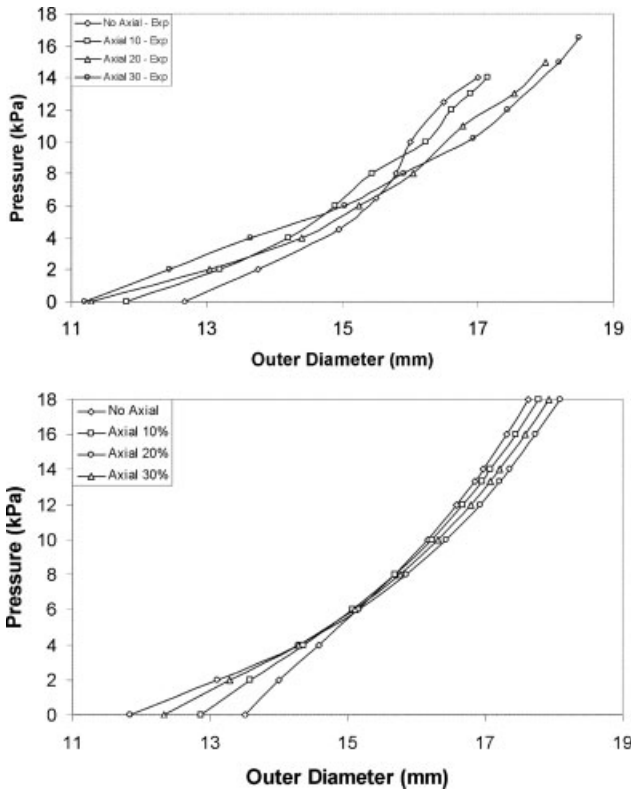

Figure 4 Comparison of the experimental and numerical inflations of a PVA–chitosan WS-1 hydrogel vessel (three freeze–thaw cycles): (A) experimental pressure versus the diameter for the hydrogel vessel with no axial strain or 10, 20, or 30% axial strain (n = 3) and (B) numerical pressure versus the diameter for the hydrogel vessel with no axial strain or 10, 20, or 30% axial strain.

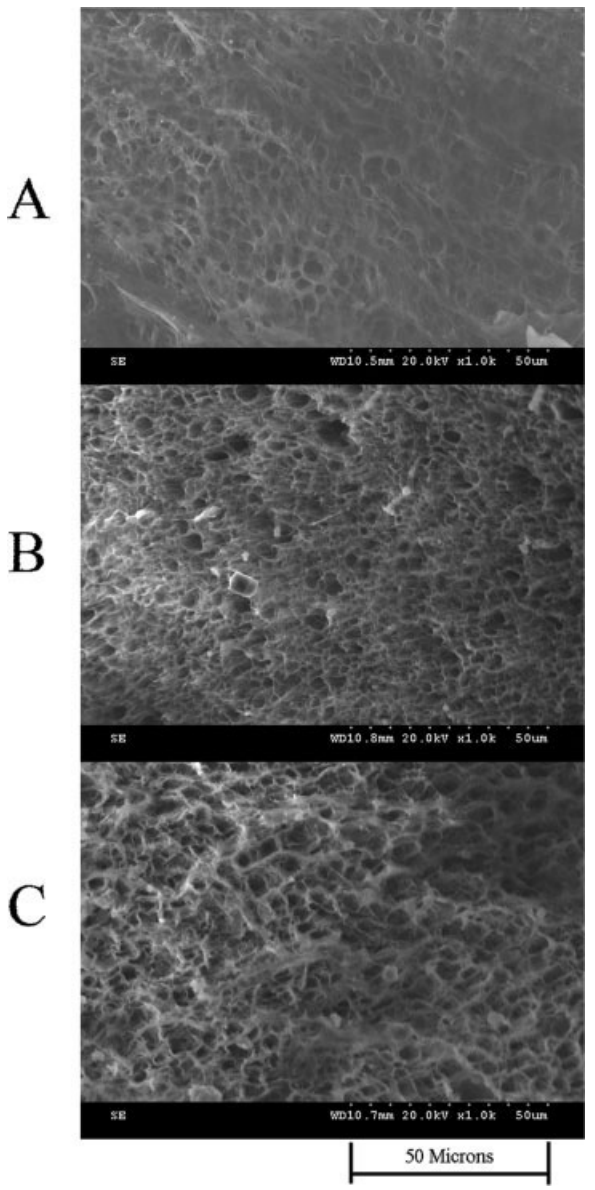

Figure 5 Cross-sectional SEM images of the dehydrated PVA membranes: (A) one freeze–thaw cycle, (B) two freeze–thaw cycles, and (C) four freeze–thaw cycles (representative images, $n = 3$, 1000× magnification).

or four freeze–thaw cycles, the specimens that underwent one freeze–thaw cycle were loaded to a maximum load of 0.3 N, whereas specimens that underwent four freeze–thaw cycles were loaded to a maximum load of 1 N at a strain rate of 60%/min. In Figure 3, it is clearly shown that the response became more compliant after the initial cycle for the PVA–chitosan WS samples subjected to one and four freeze–thaw cycles. Similar results were obtained for the IS samples. All of the membranes were most affected by the first cycle and settled into a consistent pattern as further cycles were applied. When the hydrogel membranes were conditioned, the materials tended to become more compliant at loads far below the maximum prior load, but they stiffened considerably as the load approached the original peak level.

Vessel dilation tests

Internal pressurization combined with axial elongation was used to determine the structural response of the PVA–chitosan WS-1 hydrogel tubular vessels. The external diameters of the vessels with axial strains of 0, 5, 10, and 20% were plotted at stepped increases of internal pressure. For comparison purposes, a finite element model of this experiment was constructed.

The structural response of the numerical model was compared to the experimental measurements for

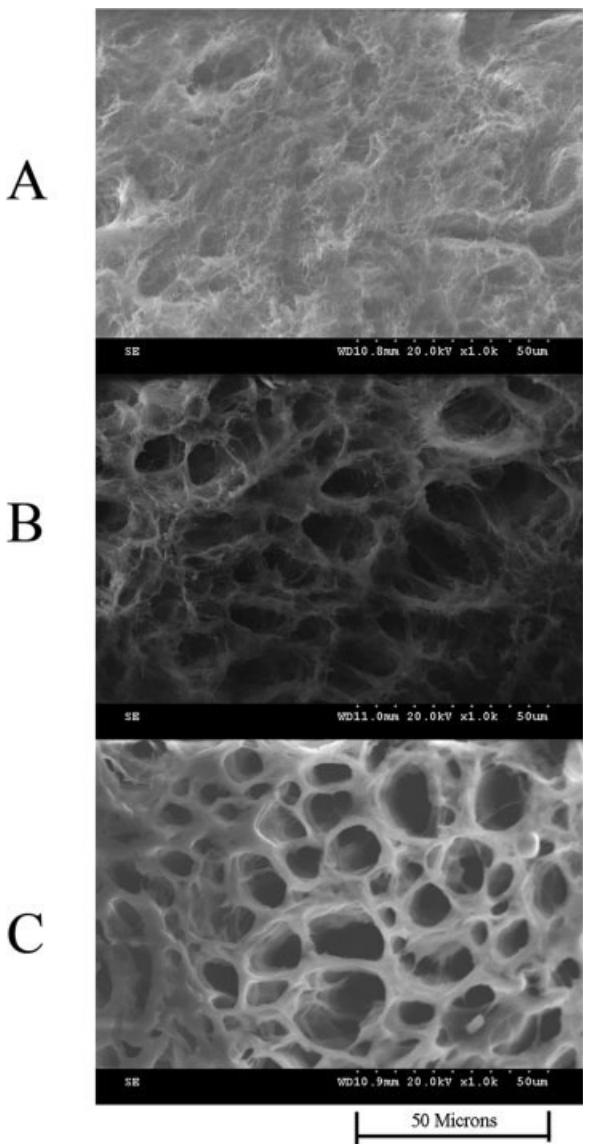

Figure 6 Cross-sectional SEM images of the dehydrated PVA–chitosan WS membranes: (A) one freeze–thaw cycle, (B) two freeze–thaw cycles, and (C) four freeze–thaw cycles (representative images, $n = 3$, 1000× magnification).

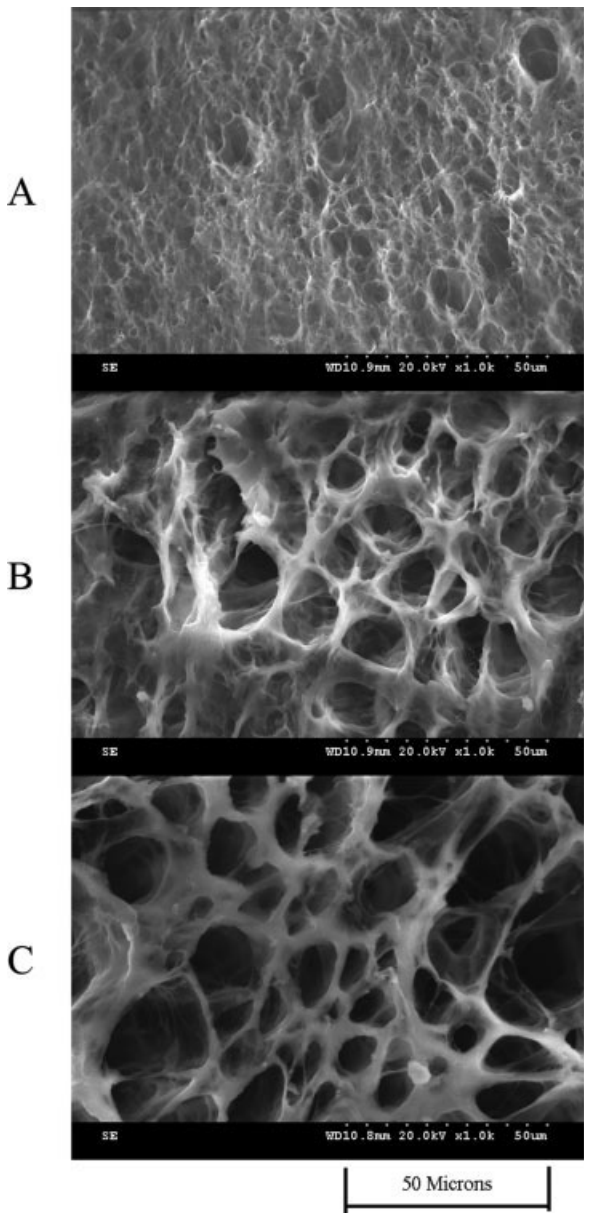

Figure 7 Cross-sectional SEM images of the dehydrated PVA–chitosan IS membranes: (A) one freeze–thaw cycle, (B) two freeze–thaw cycles, and (C) four freeze–thaw cycles (representative images, $n = 3$, 1000× magnification).

the PVA–chitosan hydrogel vessels that had undergone three freeze–thaw cycles, as shown in Figure 4. Examination of the overall experimental response of the vessels associated with specific axial strains (Fig. 4) illustrated that as the axial strain increased the unpressurized outer diameter of the vessel decreased. As the pressure was increased (above $\sim$ 8 kPa), a change in the response of the vessels was noted. Similar characteristics were also evident in the numerical model predictions (Fig. 4). Good agreement was seen between the numerical and experimental results for all of the applied extensions, which indicated that constitutive models based on the uniaxial data predicted the vessel structural behavior quite well for this load case.

SEM

Macroporous hydrogels based on the two blends of PVA with chitosan were dehydrated by freeze drying before investigation. A further hydrogel composed of 10% PVA with no chitosan was also examined. The effects of the blending of PVA with water-soluble and water-insoluble chitosan on the morphology and pore distribution were investigated by SEM. The SEM images of three hydrogel compositions, namely PVA, PVA–chitosan WS, and PVA–chitosan IS, provided high-magnification images of the cross sections of the materials. Macroscopically, all of the membranes appeared opaque. The microscopic analyses of the membranes displayed distinct differences in the composition of each of the dehydrated hydrogels for one, two, and four freeze–thaw cycles.

Figure 5 displays a porous morphology for one, two, and four freeze–thaw cycles of a pure PVA hydrogel. Larger pores were evident for one freeze–thaw cycle of PVA [Fig. 5(A)] in comparison to two freeze–thaw cycles [Fig. 5(B)]. No significant visual differences were apparent in the cross-sectional structure of the PVA between two and four freeze–thaw cycles. For all freeze–thaw cycles of PVA, an ordered structure was evident, which suggested a homogeneous structure. When water-soluble or water-insoluble chitosan was added to the PVA, significant changes were apparent in the internal structure of the hydrogel compositions (Figs. 6 and 7). A similar structural morphology for both water-soluble and water-insoluble chitosan was evident for one,

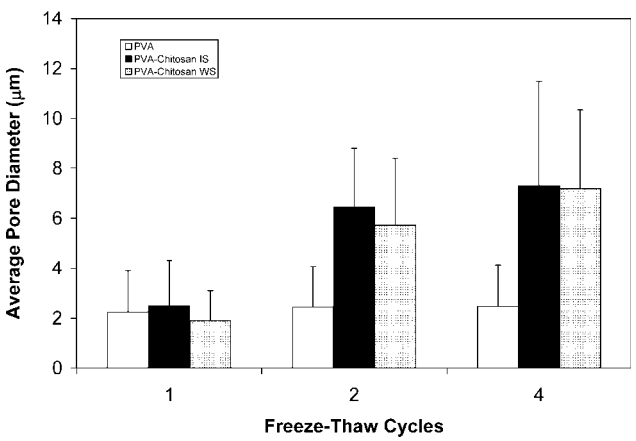

Figure 8 Average pore diameters of the PVA, PVA–chitosan IS, and PVA–chitosan WS (determined from the cross-sectional SEM images of the dehydrated hydrogel membranes with LabVIEW software, Austin, TX; $n = 3$).

TABLE II
Maximum, Minimum, and Average Pore Diameters of PVA, PVA–Chitosan IS, and PVA–Chitosan WS After One, Two, and Four Freeze–Thaw Cycles

Freeze–thaw cycles	PVA pore diameter (μm)			PVA–chitosan IS pore diameter (μm)			PVA–chitosan WS pore diameter (μm)		
	Maximum	Minimum	Average	Maximum	Minimum	Average	Maximum	Minimum	Average
1	3.68	1.61	2.24	3.71	1.95	2.50	2.69	1.15	1.90
2	3.76	1.73	2.44	11.19	2.26	6.44	11.97	2.66	5.72
4	3.80	1.67	2.47	15.19	4.16	7.29	13.75	3.12	7.19

two, and four freeze–thaw cycles. The PVA–chitosan WS and IS hydrogels that underwent one freeze–thaw cycle had a spongelike cross-sectional structure [Figs. 6(A) and 7(A)]. After two freeze–thaw cycles, larger pores were evident for both hydrogel compositions [Figs. 6(B) and 7(B)]. Finally, after four freeze–thaw cycles, the pores were of similar size to the pores after two freeze–thaw cycles but were much more clearly defined [Figs. 6(C) and 7(C)]. A histogram of the average pore diameters was generated (Fig. 8) from three 1000× cross-sectional SEM images ($n = 3$) of the dehydrated PVA, PVA–chitosan IS, and PVA–chitosan WS hydrogel membranes after one, two, and four freeze–thaw cycles. There were approximately 40 ± 15 pores per image. One representative image for each case is shown in Figures 5–7. The histogram illustrates that there was no significant difference in the average pore diameter for PVA after one, two, and four freeze–thaw cycles (2.24, 2.44, and 2.47 μm, respectively; see Table II). There was a significant increase in the average pore diameter after two freeze–thaw cycles for PVA–chitosan WS and IS membranes in comparison to the average pore diameter after one freeze–thaw cycle. Another increase in the pore diameter of the PVA–chitosan WS and IS membranes was evident after four freeze–thaw cycles in comparison to after two freeze–thaw cycles.

We concluded that both water-soluble and water-insoluble chitosan had a similar effect on the hydrogel morphological structure. SEM images of the internal PVA, PVA–chitosan WS, and PVA–chitosan IS structures showed a porous filamentous membrane, which could allow the transport of additives through the membrane. As shown in a previous publication, PVA–chitosan WS and PVA–chitosan IS support vascular cell culture, which indicates that the pore sizes in these hydrogels provide a suitable membrane for all cell growth. However, there was a marked difference in the maximum and minimum pore diameters of the PVA–chitosan WS and IS membranes (see Table II). Ideally, a biomaterial for such applications would have uniform pore architecture[25] to allow the quantification of nutrient transport through the membrane.

CONCLUSIONS

This series of experiments indicated that the addition of chitosan to PVA hydrogels affected their mechanical behavior and morphological structure. The effect of freeze–thaw cycles on the mechanical properties of PVA–chitosan WS-1 and IS-1 in a uniaxial test specimen and in a molded tubular structure were determined. The effect of conditioning during initial loading was shown to be important. The uniaxial properties were within the range of published characteristics for porcine aortic tissue.

Nonlinear hyperelastic constitutive Ogden models were used to describe the behavior of each PVA–chitosan WS membrane for one, two, three, and four freeze–thaw cycles. A numerical model of the vessel response to internal pressurization agreed well with the experimental measurements for the selected case of a three freeze–thaw cycle PVA–chitosan WS-1 hydrogel vessel.

The number of freeze–thaw cycles was shown to have a significant effect on the morphological characteristics of the PVA–chitosan WS-1 and IS-1 hydrogel membranes.

These findings, coupled with those from earlier biological evaluation studies,[19] suggest that PVA–chitosan hydrogels can be used to fabricate vessels with appropriate mechanical and structural properties for *in vitro* vascular cell culture studies in a vascular bioreactor and merit further investigation for tissue engineering applications.

References

1. Mann, B. K. Clin Plast Surg 2003, 30, 601.
2. Nuttelman, C. R.; Mortisen, D. J.; Henry, S. M.; Anseth, K. S. J Biomed Mater Res 2001, 57, 217.
3. Chu, K. C.; Rutt, B. K. Magn Reson Med 1997, 37, 314.
4. Shachar, M.; Cohen, S. Heart Fail Rev 2003, 8, 271.
5. Cascone, M. G.; Lazzeri, L.; Sparvoli, E.; Scatena, M.; Serino, L. P.; Danti, S. J Mater Sci: Mater Med 2004, 15, 1309.
6. Levenberg, S.; Langer, R. Curr Top Dev Biol 2004, 61, 113.
7. Chuang, W. Y.; Young, T. H.; Yao, C. H.; Chiu, W. Y. Biomaterials 1999, 20, 1479.
8. Schmedlen, R. H.; Masters, K. S.; West, J. L. Biomaterials 2002, 23, 4325.
9. West, J. L.; Hubbell, J. A. Macromolecules 1999, 32, 241.

10. Muller, B. U.S. Pat. 5,508,317 (1996).
11. Wan, W. K.; Campbell, G.; Zhang, Z. F.; Hui, A. J.; Boughner, D. R. J Biomed Mater Res 2002, 63, 854.
12. Jiang, H.; Campbell, G.; Boughner, D.; Wan, W. K.; Quantz, M. Med Eng Phys 2004, 26, 269.
13. Vijayasekaran, S.; Fitton, J. H.; Hicks, C. R.; Chirila, T. V.; Crawford, G. J.; Constable, I. J. Biomaterials 1998, 19, 2255.
14. Stammen, J. A.; Williams, S.; Ku, D. N.; Guldberg, R. E. Biomaterials 2001, 22, 799.
15. Cascone, M. G.; Sim, B.; Downes, S. Biomaterials 1995, 16, 569.
16. Hassan, C. M.; Stewart, J. E.; Peppas, N. A. Eur J Pharm Biopharm 2000, 49, 161.
17. Hassan, C. M.; Peppas, N. A. Macromolecules 2000, 33, 2472.
18. Chandy, T.; Sharma, C. P. Biomater Artif Cells Artif Organs 1990, 18, 1.
19. Mathews, D. T.; Birney, Y. A.; Cahill, P. A.; McGuinness, G. B. J Biomed Mater Res B 2008, 84, 531.
20. Koyano, T.; Minoura, N.; Nagura, M.; Kobayashi, K. J Biomed Mater Res 1998, 39, 486.
21. Ogden, R. W. Nonlinear Elastic Deformations; Wiley: New York, 1984.
22. Knaul, J. Z.; Creber, K. A. M. J Appl Polym Sci 1997, 66, 117.
23. Prendergast, P.; Lally, C.; Daly, S.; Reid, A. J.; Lee, T.; Quinn, D.; Dolan, F. J Biomech Eng 2003, 125, 692.
24. O'Flynn, P. M.; Roche, E. T.; Pandit, A. S. Asaio J 2005, 51, 426.
25. Hollister, S. J.; Maddox, R. D.; Taboas, J. M. Biomaterials 2002, 23, 4095.